EUROPEAN ORGANIZATION FOR NUCLEAR RESEARCH

CERN-EP/81-141
5 November 1981

MEASUREMENT OF THE ANTIPROTON-PROTON TOTAL CROSS-SECTION AND ELASTIC SCATTERING AT THE CERN INTERSECTING STORAGE RINGS

G. Carboni, G. Kantardjian and D. Lloyd-Owen*)

CERN, Geneva, Switzerland

M. Ambrosio, G. Anzivino, G. Barbarino, G. Paternoster and S. Patricelli

Istituto di Fisica dell'Università, Napoli, and INFN, Sezione di Napoli, Italy

V. Cavasinni**), T. Del Prete, M. Morganti and M. Valdata-Nappi

INFN, Sezione di Pisa and Istituto di Fisica dell'Università, Pisa, Italy

P.D. Grannis

State University of New York, Stony Brook, USA

ABSTRACT

We measured the total cross-section for $\bar{p}p$ scattering at $\sqrt{s}$ = 53 GeV at the CERN ISR. The method was based on the measurement of the total interaction rate and of the ISR luminosity. The result obtained, σ_{tot} = 44.1 ± 2.0 mb, suggests that $\sigma_{tot}(\bar{p}p)$ starts increasing at ISR energies. A measurement of the $\bar{p}p$ differential cross-section was also performed: the results show a change in the slope at $|t| \simeq 0.1$ GeV^2, similar to that observed in pp scattering.

(Submitted to Physics Letters B)

---

*) Also at State University of New York, Stony Brook, USA.

**) Also at Istituto di Fisica dell'Università, Bologna, Italy.

We have studied some global properties of antiproton-proton scattering at $\sqrt{s}$ = 53 GeV in an experiment being performed at the CERN ISR. In the first half of this letter, we shall present our measurement of the total cross-section. The second half will be devoted to our results for the differential elastic cross-section. (Results on multiplicities and single-particle distributions will be the subject of a later article.)

The total cross-section σ_{tot} was measured using the total-rate method, following the techniques developed by the Pisa-Stony Brook Collaboration [1-5]. The latter experiment and that of the CERN-Rome Collaboration [3-6] discovered that the pp total cross-section rises at high energy: as we shall see, the results of the present experiment suggest that the same is the case for $\bar{p}p$ interactions.

The total-rate method consists of the simultaneous measurement of the total interaction rate R_{tot} and the ISR luminosity L, which are related to σ_{tot} by

$$\sigma_{tot} = \frac{R_{tot}}{L} \ . \qquad (1)$$

This method was chosen because it is direct: corrections play a minor role, representing in our case some 4% of the final result.

To measure R_{tot}, a 4π detector consisting of large scintillation-counter hodoscopes was installed in intersection 2 of the ISR (Fig. 1a). Except for two narrow forward cones (totalling 1.9×10^{-4} sr), the entire solid angle around the interaction region was covered by at least two planes of trigger counters operated in coincidence.

Hodoscopes CI and CO were concentric rectangular boxes surrounding the interaction region. The hodoscopes H_1, H_2, H_3, and H_4 were roughly circular centred on the exiting vacuum chamber. The hodoscopes H_5 and TB each consisted of two rectangular planes of counters again centred on the vacuum chamber. The two arms of the detector were mirror images of each other.

A fully inclusive trigger was used for the total-rate measurement

$$T = (TB + H_5 + H_4 \cdot H_3 + H_2 \cdot H_1 + CO \cdot CI)_{left} \cdot (CI \cdot CO + H_1 \cdot H_2 + H_3 \cdot H_4 + H_5 + TB)_{right} \ ,$$

i.e. a charged particle detected in the left hemisphere in coincidence with a charged particle detected on the right was sufficient to provide a trigger.

The resolving time of the left-right trigger coincidence was intentionally kept rather wide (±40 ns) to study the main source of ISR background: jets of secondary particles produced when one of the circulating particles interacts with the residual gas in the vacuum chamber or with the vacuum chamber itself.

The jets from such "single-beam" interactions entered the apparatus from the sides and could be distinguished from true "beam-beam" events by the relative timing of hodoscopes in the left and the right arms. For each event, the timing of each hodoscope pair with respect to the trigger was recorded, i.e. five time measurements for each arm. In the off-line analysis, the events due to beam-beam interactions were separated from background by inspecting the 25 independent left-right time-of-flight differences (TOFs) that could be formed from the 10 time measurements. The discrimination between signal and background was best for those TOFs corresponding to hodoscopes far from the interaction region. Since the average detected multiplicity was high ($\simeq$ 14), the greatest majority of the events appeared in several TOFs. In those events where only the CI·CO coincidence was present in one arm, there was not sufficient resolution to discriminate against the background. Such events, however, contributed < 0.5% to the total rate.

The rate R_{obs} measured by the detector differed from the total rate R_{tot} because of the incomplete coverage at small angles*). The greatest majority of the events lost at small angles were elastic events**). This loss was evaluated by integrating an extrapolated differential cross-section over the region of the holes. This cross-section was parametrized by

$$\frac{d\sigma_{el}}{d|t|} = A \exp(-b|t|) ,$$

the parameters A and b being determined in a separate run. The correction for elastic losses is virtually insensitive to changes in these parameters because

---

*) The trigger loss caused by cracks between adjacent counters was estimated at < 1% and has not been corrected.

**) We neglected the < 0.35% loss of diffractive events.

$d\sigma_{el}/d|t|$ is fixed at $\theta = 0°$ by the optical theorem and because $b|t| \ll 1$ over the region of integration. The increment $\Delta\sigma_{el}$, used to correct for elastic losses, is listed in Table 1.

The measurement of the ISR luminosity L was achieved using a monitor calibrated in special runs by the method of Van der Meer [7]. A luminosity monitor consists of two telescopes, one in each hemisphere, operated in coincidence. If the distance of the telescopes from the interaction region is large enough, the left-right coincidence detects only beam-beam events and the monitor rate R_{mon} is proportional to L

$$R_{mon} = \sigma_{mon} L .$$

The proportionality constant σ_{mon} is the inclusive cross-section for events that trigger the monitor.

At the ISR, the value of L depends only on the beam currents and the vertical overlap of the beams. By vertically displacing the beams with respect to each other in small, precise steps and by simultaneously measuring the monitor rate and the two beam currents, the value of the luminosity can be calculated. In this way, σ_{mon} is determined and the above equation can be used to yield L at any subsequent time*).

The ideal monitor has a large σ_{mon} and detects only beam-beam events. Several luminosity monitors were investigated in order to reach a compromise between inclusivity and background rejection. Single-beam background, almost entirely from the p beam (the p current was about 30,000 times greater than the $\bar{p}$ current), heavily contaminated the TOFs between our large-angle hodoscopes. We found that the monitor

$$M = (TB + H_5 + H_3 \cdot H_4)_{left} \cdot (H_5 + TB)_{right}$$

was virtually free of background, gave a high quality rate versus beam displacement curve (Fig. 2), and had $\sigma_{mon} = 24.09 \pm 0.94$ mb. A major contribution to the error

*) See Ref. 4 for a more complete discussion of the method.

in σ_{mon} was due to the uncertainty in the $\bar{p}$ current (±10 μA). Since the $\bar{p}$ current was 306 μA, this error (3.3%) was comparable with the statistical one.

The results of the total cross-section measurement, based on a sample of about 13,000 $\bar{p}p$ events, are summarized in Table 1. The remeasurement of the pp total cross-section made using the same detector and the same analysis as for $\bar{p}p$ agrees well with previous results. The value of 44.1 ± 2.0 mb for $\sigma_{tot}(\bar{p}p)$ suggests that following the trend of other hadronic interactions, this cross-section also rises at high energy and approaches $\sigma_{tot}(pp)$ from above (Fig. 3) [5,8,9].

We now turn to the study of elastic scattering, performed for $0.01 < |t| < 0.8$ GeV^2. Two separate detectors were used to cover this t range.

For $0.01 < |t| < 0.14$ GeV^2, we used the TBy and TBz hodoscopes, located in front of the TB trigger hodoscopes (Fig. 1b). The horizontal coordinate of the triggering particle was determined by TBy, a hodoscope of "finger" scintillators, 2.5 cm wide. The vertical coordinate was measured by TBz, an array of drift tubes [10]. Each of the four arrays comprised 24 tubes, 1 cm in diameter and 30 cm in length. The drift tubes in an array were arranged in two planes of 12 each, staggered vertically to resolve up-down ambiguities.

Data were collected with the trigger

$$T = TB_{left} \cdot TB_{right} .$$

In the off-line analysis, events with counts in the large-angle hodoscopes were rejected. For the results presented in this letter, the following event-selection criteria were imposed on the small-angle hodoscopes:

i) In the arm used to determine $|t|$, the central counter of the finger stack, TBy, and only this counter had to have been fired.

ii) In both arms, at least one overlapping pair of tubes had to have been fired.

iii) The left hit point, the interaction region, and the right hit point had to be collinear.

About 15% of genuine elastic events had more than one hit point in either arm because of δ-ray production or secondary interactions. Such events were retained if criterion (iii) was satisfied by one pair of hit points.

A loss of 30% of the elastic events was caused by rejecting multiple hits in TBy -- criterion (i). Another 10% of events was lost due to dead space in TBz. To compensate for these losses, a scale factor of 1.6 ± 0.3 was applied to the data independent of $|t|$.

To measure elastic scattering in the second $|t|$ range, $0.08 < |t| < 0.8$ GeV^2, we used the scintillation-counter hodoscope, $H_5\theta$. Located directly behind the H_5 trigger hodoscope, $H_5\theta$ was divided into 8 concentric circular rings in the polar coordinate and 4 quadrants in the azimuthal coordinate.

Data were collected with the trigger

$$T = (TB + H_5 + H_4 \cdot H_3)_{left} \cdot (H_3 \cdot H_4 + H_5 + TB)_{right} ,$$

and events with counts in hodoscopes CO, H_1, or H_2 were rejected off line. The following event-selection criteria were applied to $H_5\theta$.

i) In each arm, one and only one element of $H_5\theta$ had to have been fired.

ii) The left hit point, the interaction region, and the right hit point had to be collinear.

To compensate for loss of genuine elastic events due to the stringency of criterion (i), a scale factor of 2.3 ± 0.5 was applied to the data independent of $|t|$. This factor was determined by comparing pp data collected and analysed in the same manner with the known pp elastic cross-section.

The results from both detectors for the differential elastic cross-section $d\sigma_{el}/d|t|$ are presented in Fig. 4 and Table 2. A change in the slope parameter b occurs at $|t| \simeq 0.1$ GeV^2 for $\bar{p}p$ as for pp [11,13]. Below and above this $|t|$ value, the slope parameters for $\bar{p}p$ are equal within the errors to those for pp. From Fig. 4, it is seen that this is consistent with the trend of lower-energy data [5,13].

Extrapolating the elastic cross-section to $\theta = 0°$, we invoked the optical theorem to extract the total cross-section. We assumed that the real part of the forward amplitude was zero. The values obtained for $\sigma_{tot}(\bar{p}p)$ and $\sigma_{tot}(pp)$ in this manner are listed in Table 2. They are consistent with the values that we obtained directly, but have larger errors owing mainly to the uncertainty in the scale factor used to correct for losses.

Acknowledgements

We thank U. Becker and M. Steuer for help in the early setting-up of the experiment. The technical support from G. Barnini, A. Donnini, L. Giacomelli, T. Regan and from the technical staff of the University of Naples is gratefully acknowledged. We are indebted to the ISR staff, and especially to K. Potter, for their important contribution to this experiment.

REFERENCES

[1] S.R. Amendolia et al., Phys. Lett. 44B, 119 (1973).

[2] S.R. Amendolia et al., Nuovo Cimento 17A, 735 (1973).

[3] U. Amaldi et al., Phys. Lett. 62B, 460 (1976).

[4] U. Amaldi et al., Nucl. Phys. 145B, 367 (1978).

[5] G. Giacomelli and M. Jacob, Phys. Rep. 55, 1 (1979).

[6] U. Amaldi et al., Phys. Lett. 44B, 112 (1973).

[7] S. Van der Meer, CERN Internal Report ISR-PO/68-31 (1968).

[8] J.G. Rushbrooke and B.R. Webber, Phys. Rep. 44, 2 (1978).

[9] K.R. Schubert, Tables on nucleon-nucleon scattering, *in* Landolt-Börnstein, Numerical Data and Functional Relationships in Science and Technology (Springer, Berlin, 1980), New Series, Vol. 9.

[10] U. Becker et al., Nucl. Instrum. Methods 180, 61 (1981).

[11] G. Barbiellini et al., Phys. Lett. 39B, 663 (1972).

[12] D. Favart et al., Phys. Rev. Lett. 47, 1191 (1981).

[13] U. Amaldi, M. Jacob and G. Matthiae, Ann. Rev. Nucl. Sci. 26, 385 (1976).

Table 1

Summary of results on total cross-section

$\sqrt{s}$ (GeV)	Reaction	Detected cross-section σ_{obs} (mb)	Increment for elastic loss $\Delta\sigma_{el}$ (mb)	Total cross-section σ_{tot} (mb)
53 a)	$p\bar{p}$	42.4 ± 2.0	1.7 ± 0.2	44.1 ± 2.0
53 a)	pp	40.7 ± 0.4	1.7 ± 0.2	42.4 ± 0.4
53 b)	pp			42.71 ± 0.35

a) This experiment.

b) Ref. 4.

Table 2

Summary of results on the elastic scattering
$d\sigma_{el}/dt \propto \exp(-b|t|)$

$\sqrt{s}$ (GeV)	Reaction	b_1 a) (GeV^{-2})	b_2 b) (GeV^{-2})	Total cross-section σ_{tot} c) (mb)
53 d)	$p\bar{p}$	14.0 ± 2.6	10.4 ± 0.6	41.5 ± 4.0
53 d)	pp	12.6 ± 1.4	10.4 ± 0.4	43.9 ± 4.0
53 e)	pp	13.1 ± 0.2		42.38 ± 0.27
53 f)	pp		10.8 ± 0.2	
53 g)	$p\bar{p}$	13.6 ± 2.2		44.1 ± 2.9

a) $b_1 = b$ for $|t| < 0.1$ GeV^2.

b) $b_2 = b$ for $|t| > 0.1$ GeV^2.

c) From the optical theorem.

d) This experiment.

e) Ref. 4.

f) Ref. 11.

g) Ref. 12.

Figure captions

Fig. 1 : a) Schematic layout of the experiment: CI, CO, H_1, H_2, H_3, H_4, H_5, and TB are scintillation-counter hodoscopes.

b) Exploded view of the TB small-angle hodoscope:

TBϕ = double layer of trigger counters;

TBy = "finger" counter stack;

TBz = staggered arrays of drift tubes.

Fig. 2 : Luminosity curve: the monitor rate versus the vertical separation δ of the ISR beams. The integral of this curve, together with the values of the beam currents, yields the cross-section of the monitor.

Fig. 3 : The results of $\sigma_{tot}(pp)$, $\sigma_{tot}(p\bar{p})$, and of the difference $\sigma_{tot}(pp) - \sigma_{tot}(p\bar{p})$ are displayed versus equivalent laboratory momentum P_{lab}.

Fig. 4 : The differential elastic cross-section for $p\bar{p}$ at $\sqrt{s}$ = 53 GeV. The low $|t|$ data are shown expanded in the upper inset. The value of the slope parameter for $\langle|t|\rangle = 0.2$ GeV^2 is shown in the lower inset; other data are shown for comparison.

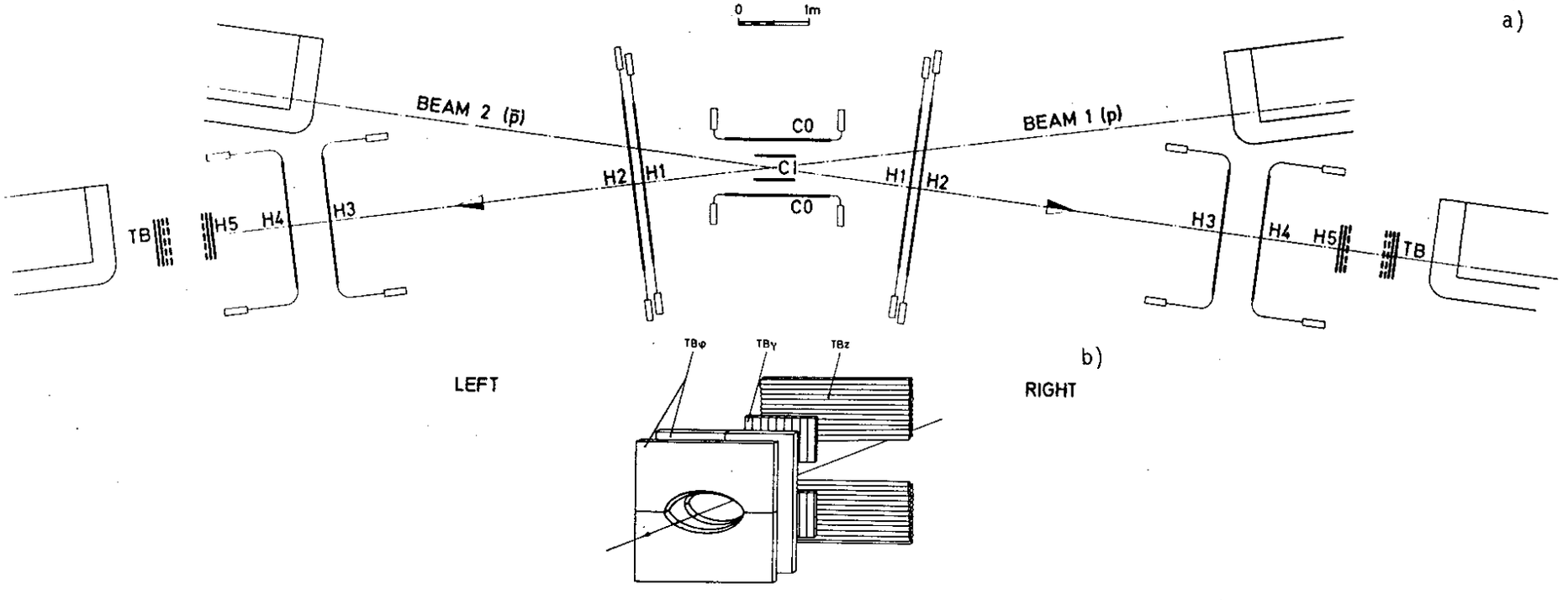
0
1m
a)
BEAM 2 ($\bar{p}$)
BEAM 1 (p)
C0
C
C0
H2
H1
H1
H2
TB
H5
H4
H3
H3
H4
H5
TB
TBφ
TBγ
TBz
b)
LEFT
RIGHT

Fig. 1

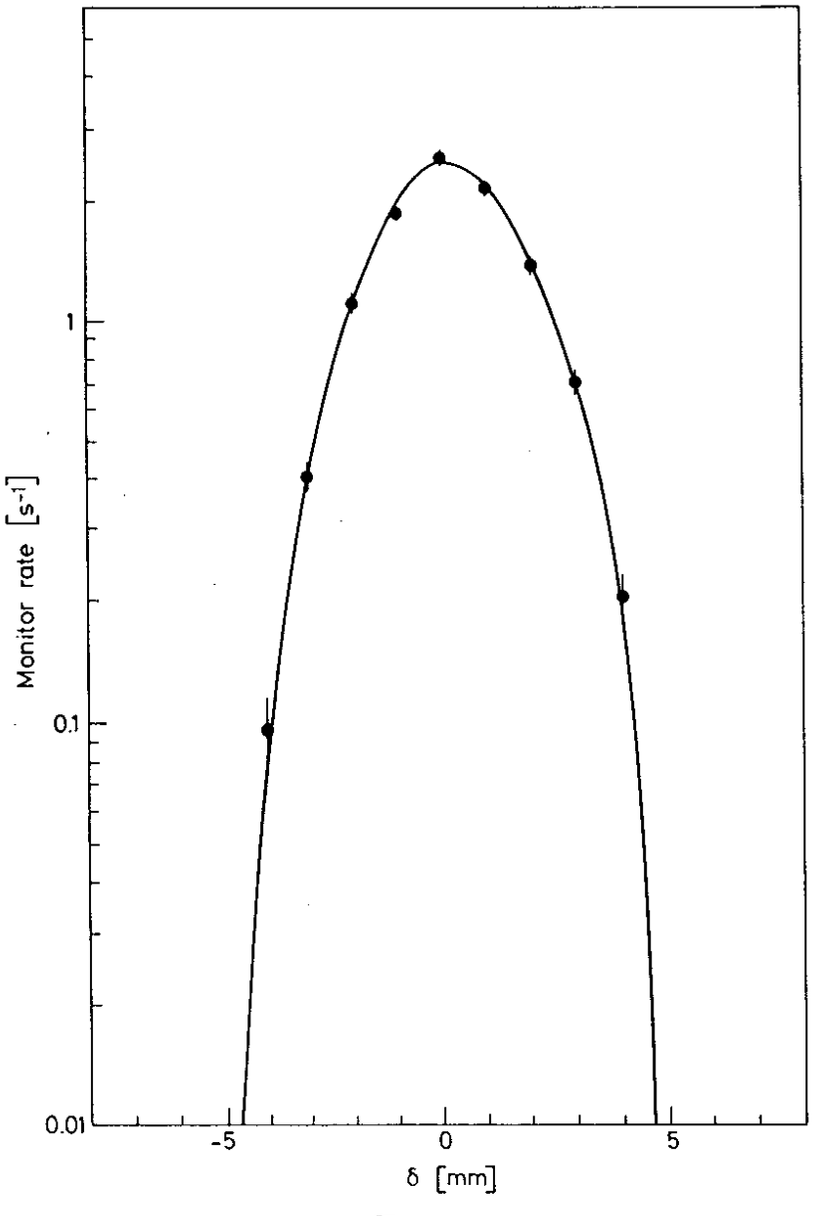
Monitor rate [s⁻¹]
1
0.1
0.01
-5
0
5
δ [mm]

Fig. 2

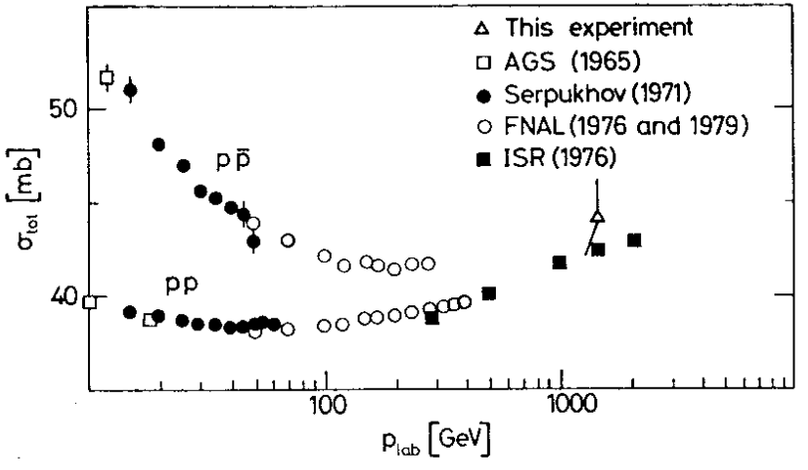
This experiment
AGS (1965)
Serpukhov (1971)
FNAL (1976 and 1979)
ISR (1976)
pp̄
pp
σtot [mb]
50
40
100
1000
plab [GeV]

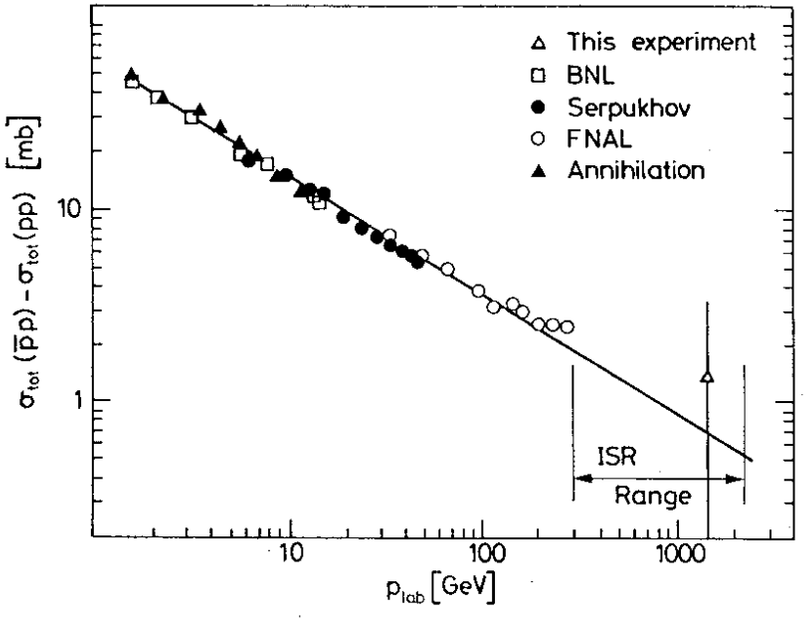
This experiment
BNL
Serpukhov
FNAL
Annihilation
σtot (p̄p) - σtot (pp) [mb]
10
1
ISR
Range
10
100
1000
plab [GeV]

Fig. 3

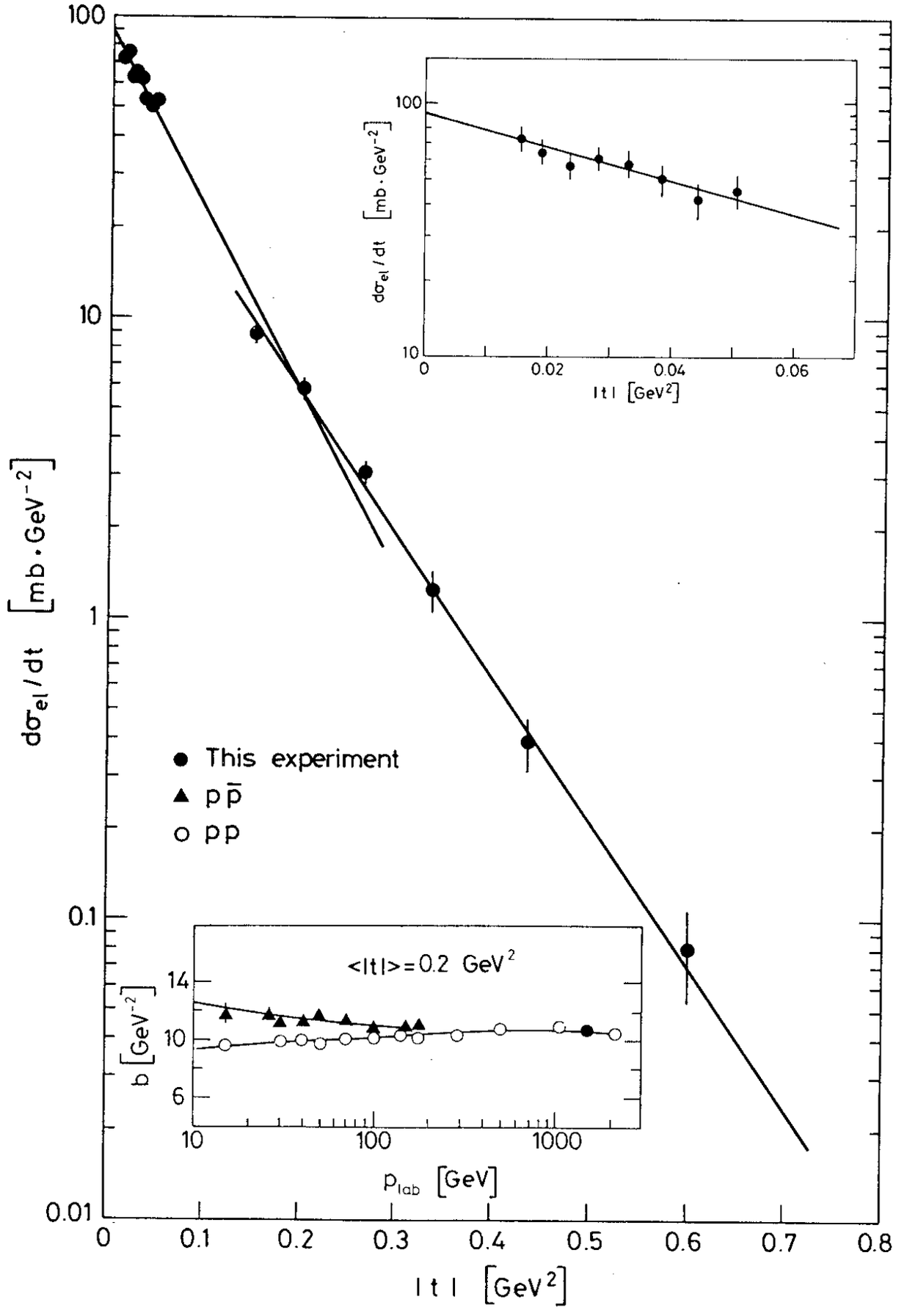
100
10
1
0.1
0.01
0
0.1
0.2
0.3
0.4
0.5
0.6
0.7
0.8
dσel/dt [mb·GeV-2]
|t| [GeV2]
● This experiment
▲ p p̄
○ pp
100
10
0
0.02
0.04
0.06
dσel/dt [mb·GeV-2]
|t| [GeV2]
<|t|>=0.2 GeV2
14
10
6
b [GeV-2]
10
100
1000
plab [GeV]

Fig. 4